JOURNAL OF CATALYSIS 135, 533–547 (1992)

Potassium Promotion of Iron Oxide Dehydrogenation Catalysts Supported on Magnesium Oxide

1. Preparation and Characterization

D. E. STOBBE,* F. R. VAN BUREN,* A. J. VAN DILLEN,† AND J. W. GEUS†

*Dow Benelux N.V., P.O. Box 48, 4530 AA Terneuzen, The Netherlands; and
†Department of Inorganic Chemistry, State University of Utrecht, P.O. Box 80083, 3508 TB Utrecht, The Netherlands

Received October 3, 1990; revised September 13, 1991

Catalysts of iron oxide supported on magnesium oxide and promoted with potassium were prepared by incipient wetness impregnation of preshaped magnesium oxide support pellets with a solution of an iron complex, either ammonium iron(III) citrate or ammonium iron(III) EDTA and potassium carbonate. Iron and potassium were applied either simultaneously or consecutively. As determined using X-ray diffraction, thermogravimetric analysis, and magnetic measurements, calcination above 923 K results in the formation of a mixed oxide of iron and potassium, viz., $KFeO_2$. After calcination at 973 K the average crystallite size of the $KFeO_2$ phase is about 300 Å. The formation of $KFeO_2$ appeared to have a strong retarding effect on the reduction of the iron oxide phase to metallic iron. It was found that the $KFeO_2$ phase is unstable in atmospheric air due to reaction with carbon dioxide and moisture to form potassium (hydrogen)carbonate and (hydrated) iron oxide.

INTRODUCTION

Magnesia-supported iron oxide catalysts promoted with potassium are being developed for dehydrogenation reactions such as the dehydrogenation of ethylbenzene or 1-butene (*1*). With the conventional unsupported iron oxide catalysts used in the dehydrogenation of ethylbenzene, deterioration of the mechanical strength of the catalysts presents problems. The use of a magnesium oxide-supported iron oxide catalyst is expected to be favorable for maintaining the mechanical strength during operation.

Previously, it has been established that unpromoted iron oxide catalysts supported on magnesium oxide deactivate due to carbon deposition under process conditions (*2*). According to the literature, this is a common feature of unpromoted dehydrogenation catalysts based on iron oxide (*3, 4*). Alkali compounds, such as potassium carbonate and potassium hydroxide, are added to these catalysts to suppress coking (*5–7*). Potassium carbonate is known as an especially effective catalyst in carbon gasification (*8*).

Next to catalyzing carbon gasification, alkali compounds are often reported to have a strong promoting effect in a wide variety of heterogeneously catalyzed hydrocarbon manufacturing processes (*9*). More specifically, in ethylbenzene dehydrogenation, potassium increases the activity of unsupported iron oxide catalysts by over an order of magnitude (*10*). In the past, several concepts have been proposed to explain this phenomenon. Lee and Holmes (*11*) supposed that potassium increases activity by encouraging electron transfer at the solid–gas interface. According to Vijh (*12*), the promoting power of various alkali and alkali earth metal oxides is correlated to their ionicity. The catalysts have active sites located on or around points on the catalyst surface where the promoter atoms are em-

0021-9517/92 $5.00

bedded. Mross (*9*) even considered the catalyst as a two-phase mixture of solid magnetite and a supported liquid film of potassium hydroxide, i.e., the supported liquid phase model. More recently, however, a trend has developed in which the active phase is considered to be constituted of mixed oxides of potassium and iron (*13, 14*). This seems to be in contradiction with the generally observed reduction of iron oxide to Fe_3O_4 under process conditions (*10, 15*). It is known that magnetite does not form a ternary phase with potassium because of the unfavorable size of the K^+ ion (*16*). Nevertheless, Shibata and Kiyoura (*17*) ascribed the promoting effect of potassium to the formation of $K_2Fe_{22}O_{34}$. Others hold the view that the active phase consists of $KFeO_2$ (*18–20*). $K_2Fe_{12}O_{19}$ has also been reported to be an active phase (*21*).

The present paper deals with the preparation and characterization of iron oxide catalysts supported on magnesium oxide promoted with potassium carbonate. Special attention is paid to solid-state reactions occurring in the course of the preparation with emphasis on the possible formation of mixed oxides of potassium and iron. In a previous paper, it has been shown that magnesium ferrite in unpromoted supported iron oxide catalysts is reduced under dehydrogenation conditions (*2*). Generally, reduction of the iron oxide phase is reported for unsupported iron oxide catalysts as well (*10, 15*). Therefore, the reduction behavior of the supported iron oxide catalysts after promotion with potassium has been studied in detail. To characterize the catalysts and to assess the species obtained upon reduction, a wide variety of techniques has been used. These include X-ray diffraction (XRD), thermogravimetric analysis (TGA), high-field magnetization measurements (TMA), and temperature-programmed reduction experiments (TPR). The influence of the potassium promoter on the catalytic activity and stability in 1-butene dehydrogenation will be dealt with in the succeeding paper (Part 2) (*22*).

EXPERIMENTAL

Catalyst Preparation

Magnesia-supported iron oxide catalysts promoted with potassium were prepared either by consecutive impregnation of preshaped magnesium oxide support pellets with solutions of an iron complex and potassium carbonate or by simultaneous impregnation of the support with a solution containing both compounds. As support, preshaped magnesium oxide support pellets (Engelhard, Mg-0601 T $\frac{1}{8}$ in.) were used with a specific surface area of 8.2 m^2/g. The cumulative pore volume of the magnesium oxide support was 0.346 cm^3/g.

With consecutive application, the magnesium oxide support was impregnated using the incipient wetness procedure with an iron precursor, such as ammonium iron(III) citrate (BakerGrade) or ammonium iron(III) EDTA (Merck, Fotopur) (*23*). The catalyst was dried in air for 24 h at room temperature, followed by drying in air at 393 K for another 24 h. Subsequently, the catalyst was calcined at 973 K in air for 24 h. Air used for the calcination was dried over a molecular sieve (Linde 4A). Next, the evacuated catalyst was impregnated to incipient wetness with a solution of potassium carbonate (Merck, p.a.) in water. The promoted catalyst was dried and calcined following the procedure described above. Calcination was also performed at 973 K, unless specified otherwise.

Catalysts were also prepared by simultaneous impregnation with an iron complex and potassium carbonate. For this purpose a solution containing both an iron complex and potassium carbonate was prepared. The evacuated preshaped magnesium oxide support pellets were impregnated to incipient wetness, after which the catalyst was dried and calcined following the procedure described above for the consecutive method. Typical loadings varied between 1 and 3 wt% Fe and between 1 and 6 wt% K expressed as weight percentage of the elements on the magnesium oxide support.

Characterization Techniques

X-ray diffraction measurements were performed in a Philips powder diffractometer mounted on a Philips PW-1140 X-ray generator with Fe$K\alpha_{1,2}$ radiation (λ = 1.93735 Å).

High-field magnetic measurements were performed using a modification of the Weiss extraction technique described earlier (*24, 25*). Thermomagnetic analyses were performed at a field strength of 0.39 MA/m in helium. Before use helium was purified over activated cabon at liquid nitrogen temperature. The amounts of catalyst used were chosen so as to contain roughly equal amounts of iron for each analysis. Previously, the catalyst pellets were fragmented into particles of sizes between 0.5 and 0.85 mm.

The reduction behavior was studied by temperature-programmed reduction. Experiments were performed in a conventional atmospheric flow reactor, as described previously (*26*). Hydrogen consumption, which was determined as a function of the temperature, was monitored continuously using a thermal conductivity detector both before and after the reactor. Product water was frozen out using a cold trap, usually CO_2(s)/CO_2(g), 194 K, or occasionally ethanol(s)/ethanol(l), 156 K. Amounts of about 150 mg of catalyst were reduced in a 10% H_2/Ar flow. The flow rate was about 100 ml/min. The temperature was raised linearly at a rate of 0.06 K/s.

Thermogravimetric analysis (DuPont 951-TGA cell coupled to a DuPont 2100 unit) was performed in an air flow at a heating rate of 5 K/min.

The catalysts were also characterized using a scanning electron microscope (Cambridge Stereoscan 150), which was equipped with an X-ray microanalyzer (Link system).

RESULTS AND DISCUSSION

Catalyst Preparation

Scanning electron microscopy. In a previous paper it has been shown that impregnation of magnesium oxide pellets with an aqueous solution of ammonium iron(III) citrate or ammonium iron(III) EDTA results in a homogeneous distribution of the iron throughout the preshaped support pellets (*23*). In this work, the potassium distribution is also of interest. The potassium distribution throughout the catalyst pellets after drying and calcination has been determined using X-ray microanalysis. Typical potassium $K\alpha$ linescans and the corresponding backscatter electron images (BEI) of 3 wt% Fe/3 wt% K/MgO catalysts are shown in Fig. 1. Impregnation of preshaped magnesium oxide with a solution containing both potassium carbonate and an iron precursor, followed by drying and calcination, i.e., the simultaneous procedure, results in a homogeneous distribution of the potassium compound throughout the pellets. The consecutive procedure also leads to a homogeneous radial distribution of potassium throughout the catalyst pellets; in this case, however, grayish potassium-rich salt deposits are found on the outer surface of the catalyst pellets, as is shown in Fig. 2. X-ray diffraction has revealed the presence of potassium sulfate, K_2SO_4. The sulfate originates from the support. As reported earlier, the support contains ca. 0.9 wt% S, which originally is present as $MgSO_4$ (*26, 27*). Whereas the unpromoted catalysts are beige after calcination at 973 K due to the formation of magnesium ferrite (*23*), the potassium-promoted catalysts are homogeneously greenish-beige after calcination. This is the case for both the simultaneously and the consecutively impregnated catalysts.

X-ray diffraction. After impregnation and drying, the potassium-promoted supported iron oxide catalysts were studied with X-ray diffraction. Figure 3 shows the X-ray diffraction patterns of a 3 wt% Fe/MgO catalyst promoted with 3 wt% K using the consecutive method. The diffractograms were recorded immediately after drying at 393 K (A), calcination at 873 K (B), and calcination at 973 K (C) in air for 24 h. After drying at 393 K, the presence of $Mg(OH)_2$ shows that the magnesium oxide support is par-

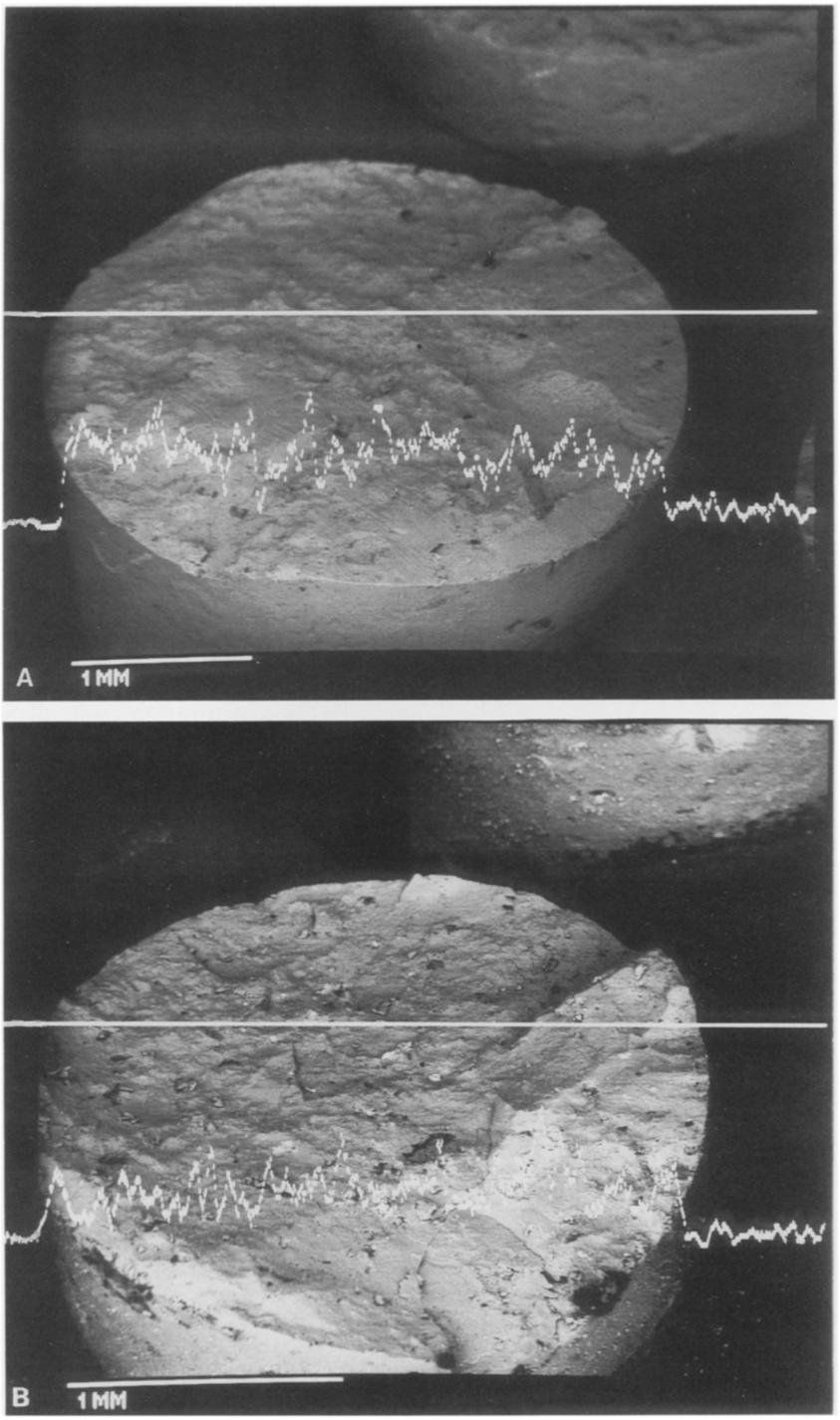

FIG. 1. Potassium $K\alpha$ linescans and the corresponding backscatter electron images (BEI) of the fracture surfaces of 3 wt% Fe/3 wt% K/MgO catalyst pellets. The solid line indicates the line along which the analysis has been performed. Bar indicates 1 mm. (A) Simultaneously impregnated, (B) consecutively impregnated.

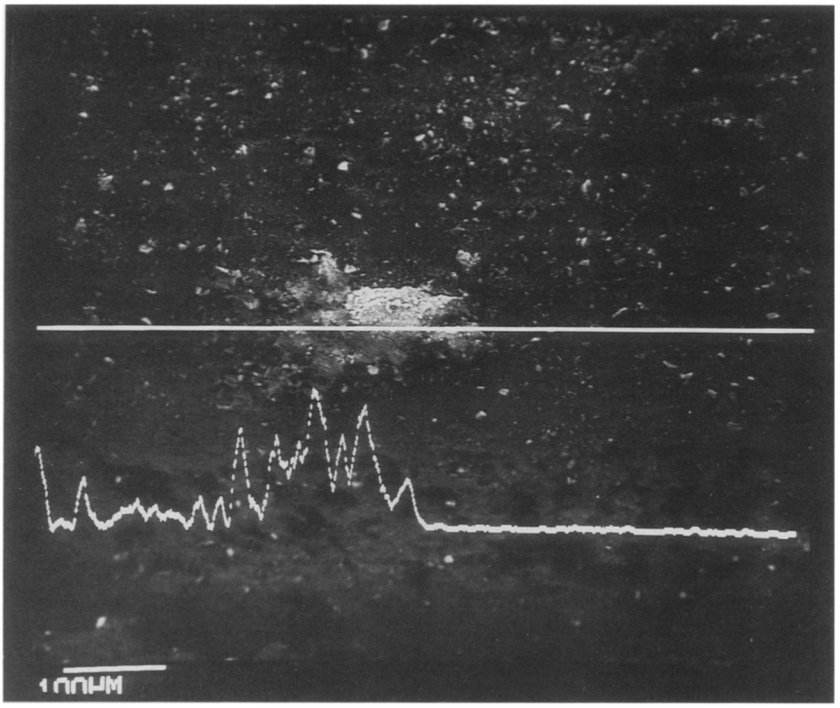

FIG. 2. Backscatter electron image and a potassium $K\alpha$ linescan of potassium-rich salt deposits present on the outer surface of a 3 wt% Fe/3 wt% K/MgO catalyst pellet prepared by consecutive impregnation. The solid line indicates the line along which the analysis has been performed. Bar indicates 100 μm.

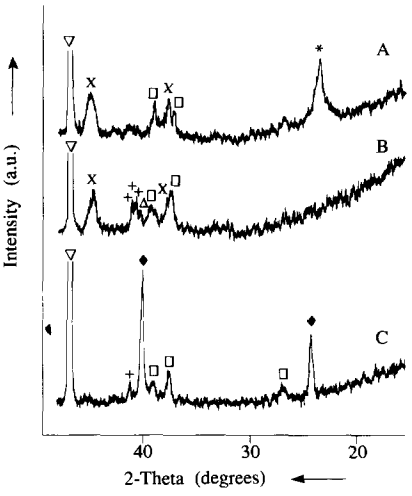

FIG. 3. X-ray diffractograms of a 3 wt% Fe/MgO catalyst promoted with 3 wt% K using the consecutive method and calcined at various temperatures. (A) 393 K, (B) 873 K, (C) 973 K. (▽) MgO, (*) $Mg(OH)_2$, (X) $MgFe_2O_4$, (□) K_2SO_4, (+) $K_2CO_3 \cdot \frac{3}{2}H_2O$, (△) K_2CO_3, (◆) $KFeO_2$.

tially hydroxylated during impregnation with an aqueous solution. In the unpromoted catalyst the iron is present as $MgFe_2O_4$. This has not changed upon impregnation with potassium carbonate. In addition to $MgFe_2O_4$, K_2SO_4 is also present in crystalline form. Potassium carbonate is not detected. After calcination at 873 K the magnesium hydroxide has decomposed, as is to be expected. In addition to magnesium ferrite and potassium sulfate, potassium carbonate is also found. It is present both in anhydrous form, K_2CO_3 and in hydrated form, $K_2CO_3 \cdot \frac{3}{2}H_2O$, probably as a consequence of rapid rehydration. Evidently, potassium carbonate must already have been present in the catalyst after drying at 393 K, but not in a crystalline form. A drastic change in the diffractogram is observed after calcination at 973 K: The potassium sulfate is still present, but the magnesium ferrite

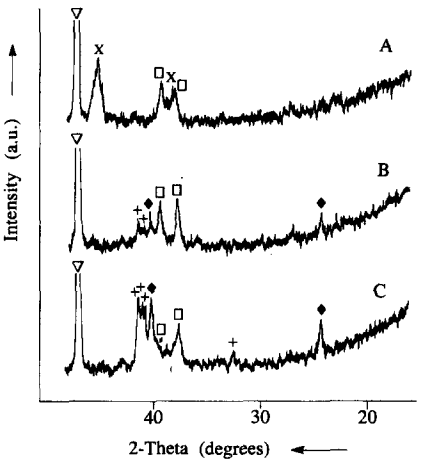

FIG. 4. X-ray diffractograms of a 3 wt% Fe/MgO catalyst consecutively promoted with different amounts of potassium. The catalysts have been calcined at 973 K. (A) 1 wt% K, (B) 3 wt% K, (C) 6 wt% K. (▽) MgO, (X) $MgFe_2O_4$, (□) K_2SO_4, (+) $K_2CO_3 \cdot \frac{3}{2}H_2O$, (◆) $KFeO_2$.

diffractions have disappeared completely. Also the potassium carbonate diffractions have become weaker. At the same time two new diffractions have appeared. According to Pistorius and de Vries (*28*) these diffractions can be ascribed to potassium ferrite, $KFeO_2$. For a long time this compound was erroneously considered to display a cubic cristobalite-like structure (*18, 29*). However, Pistorius and de Vries (*28*) showed that the $KFeO_2$ structure is pseudo-cubic orthorhombic. The average crystallite size as determined using X-ray line broadening is about 300 Å.

Evidently, at 973 K magnesium ferrite must have reacted with the potassium compounds to form $KFeO_2$ particles. Since potassium sulfate is clearly more thermostable than potassium carbonate (*30*), potassium ferrite is expected to have been formed from magnesium ferrite and potassium carbonate.

The results presented thus far were obtained for catalysts prepared by consecutive impregnation with an iron complex and potassium carbonate. Results for catalysts prepared by simultaneous impregnation of potassium and iron are similar with the exception that the formation of $KFeO_2$ is observed already at 873 K.

Next, the ratio between the iron and the potassium loading of the catalysts was varied. X-ray diffractograms of catalysts containing 3 wt% Fe promoted with 1, 3, and 6 wt% K using the consecutive application procedure are shown in Fig. 4. All catalysts were finally calcined at 973 K in air, after which the XRD profiles were recorded immediately. The catalyst containing only 1 wt% K (A) does not show the presence of $KFeO_2$. Evidently, the potassium ferrite is either too dispersed or the amount formed was too small to show any diffractions. Moreover, about 1 wt% potassium is involved with the formation of potassium sulfate. Instead magnesium ferrite is still observed together with potassium sulfate. As the potassium loading is increased up to 3 wt% (B), the magnesium ferrite diffractions disappear. At the same time small diffractions of both potassium ferrite and potassium carbonate become apparent. The stoichiometric transformation of magnesium ferrite to potassium ferrite in a catalyst containing 3 wt% Fe would require a potassium loading of 2 wt% K. With 3 wt% K therefore all magnesium ferrite is expected to have disappeared and to have been converted into potassium ferrite. Nevertheless, increasing the potassium loading up to 6 wt% (C) results in an increase of the $KFeO_2$ diffraction intensity. Evidently, with only 3 wt% K, the solid-state transformation of magnesium ferrite into potassium ferrite has not been completed. With solid-state reactions, the interfacial contact area between two reactants is generally a rate-limiting factor. Obviously, an excess of potassium carbonate is required to render the solid-state reaction complete. The excess of potassium is observed in Fig. 4C as $K_2CO_3 \cdot \frac{3}{2}H_2O$ (presumably due to rapid rehydration). In all catalysts the amount of sulfate remains nearly constant, indicating that indeed the $KFeO_2$ is formed by reaction of magnesium ferrite with potassium carbonate and not by

reaction with the more stable potassium sulfate.

X-ray diffraction is not a very suitable technique for studying solid-state reactions in catalysts with relatively low loadings, due to the poor sensitivity and the requirement of crystallinity. For this reason the catalysts have also been studied magnetically.

Thermomagnetic analysis. The catalysts were studied magnetically both before and after potassium promotion using a modified Weiss extraction technique (*24, 25*). As discussed before, this technique allows for an accurate discrimination between different iron species (*26*). The thermomagnetic analysis diagram of an unpromoted catalyst containing 5.6 wt% Fe supported on magnesium oxide is shown in Fig. 5. The magnetization has been measured first at increasing and subsequently at decreasing temperatures. As can be deduced from the Curie temperature at 595 K that is observed in the TMA curve of the unpromoted catalyst (A), the iron oxide is present as ferrimagnetic magnesium ferrite (*31*). The Curie temperature is indicated by the dashed line. The solid curve indicates the signal of the empty reactor. After promotion of a 3 wt% Fe/MgO catalyst with 3 wt% K, the magnetization has decreased to values close to those measured for the empty reactor. Evidently, nearly all magnesium ferrite has been converted into a compound showing no magnetization. X-ray diffraction has revealed that this compound is $KFeO_2$. In the literature, however, no data for the magnetic characteristics of $KFeO_2$ have been found. Comparable compounds, such as KFe_5O_8 and $KFe_{11}O_{17}$, are antiferro- and antiferrimagnetic compounds, respectively (*31*). The lack of magnetization after formation of $KFeO_2$ indicates that $KFeO_2$ is likely to be an antiferromagnetic compound as well. In the TMA diagram of the catalyst promoted with 3 wt% K, the remaining signal therefore originates from a slight amount of unreacted ferrimagnetic magnesium ferrite. Due to the low magnetization the Curie temperature at 595 K can no longer be clearly distinguished. From the ratio between the magnetization at room temperature of the unpromoted catalyst and the catalyst promoted with potassium, a degree of conversion of $MgFe_2O_4$ into $KFeO_2$ of about 90% can be calculated. The magnetization of the promoted catalyst measured at room temperature at the end of the TMA is somewhat lower than the magnetization measured at the beginning. This can be explained by the fact that, as yet, some of the remaining magnesium ferrite has reacted to potassium ferrite during the TMA at high temperatures.

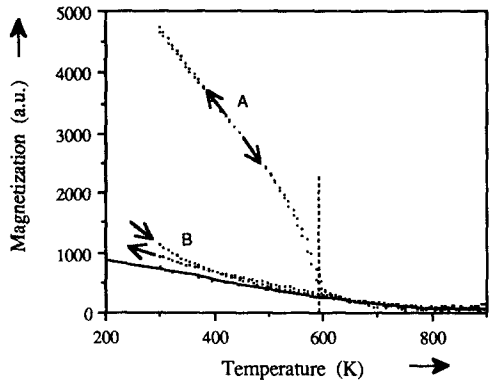

FIG. 5. Thermomagnetic analysis (TMA) diagram in helium. The solid curve indicates the signal of the empty reactor. The dashed line indicates the Curie temperature. The amounts of catalyst used have been chosen so as to contain roughly equal amounts of iron. Catalysts have been calcined at 973 K. (A) 5.6 wt% Fe/MgO catalyst, unpromoted; (B) 3.0 wt% Fe/MgO catalyst, promoted with 3.0 wt% K.

Thermogravimetric analysis. To establish the stoichiometry and the temperature range in which the transformation of magnesium ferrite into potassium ferrite proceeds, thermogravimetric analysis is the obvious technique. However, since the supported catalysts contain such low loadings of iron and potassium, the expected weight changes would be negligible. Therefore, thermogravimetric analysis has been performed on the bulk compounds. Bulk magnesium ferrite was prepared from ammonium iron(II) sulfate and magnesium sulfate by coprecipitation followed by calcination at 973 K (*32*). To study the solid-state transformations

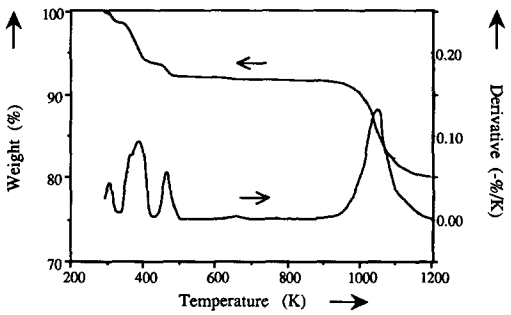

FIG. 6. Thermogravimetric analysis of a 1 : 1 (wt/wt) $MgFe_2O_4/K_2CO_3$ mixture performed in air at a heating rate of 5 K/min.

within the binary system magnesium ferrite/potassium carbonate thermogravimetric analysis has been performed in air on a 1 : 1 (wt/wt) mixture of magnesium ferrite and potassium carbonate. The thermogravimetric analysis diagram is shown in Fig. 6. Two regions of major weight loss are observed. In the first region below 500 K three small weight losses are observed at 308, 391, and 467 K. Their combined weight loss amounts to 7.57 wt% and is attributed to loss of physically and chemically adsorbed water. A second large weight loss of 11.63 wt% occurs in the region between 923 and 1123 K. This weight loss is attributed to the reaction between magnesium ferrite and potassium carbonate to form $KFeO_2$ with simultaneous evolution of CO_2:

$$MgFe_2O_4 + K_2CO_3 \rightarrow 2KFeO_2 + MgO + CO_2\uparrow \quad (1)$$

For this reaction between magnesium ferrite and anhydrous potassium carbonate a weight loss of 11.04 wt% would be expected. However, the sample initially contained 7.57 wt% water. After correction for the water content the expected weight loss for formation of $KFeO_2$ is 11.94 wt%, which is in very good agreement with the observed weight loss of 11.63 wt%.

To determine which phases have appeared or disappeared during the thermogravimetric analysis, X-ray diffraction has been performed on both the fresh bulk mixture merely dried at 393 K and the mixture after calcination at 1073 K in air, which is analogous to the treatment in the TGA experiment. The results are shown in Fig. 7. Figure 7A represents the uncalcined mixture. Diffractions of $MgFe_2O_4$, $K_2CO_3 \cdot \frac{3}{2}H_2O$, and K_2CO_3 are present, as well as those of K_2SO_4. In this case the sulfate originates from the bulk magnesium ferrite prepared by coprecipitation from the corresponding sulfates. Evidently, sulfate is difficult to remove from the precipitate by washing. Upon calcination at 1073 K in air the color of the mixture turns to olive-green, which is characteristic of $KFeO_2$ (*33*). Indeed the magnesium ferrite diffractions have almost vanished, whereas a large number of $KFeO_2$ diffractions have appeared, as shown by Fig. 7B. At the same time potassium carbonate diffractions have practically disappeared. Only a small diffraction shoulder of anhydrous potassium carbonate remains. These observations confirm once more that the weight loss between 923 and 1123 K is related to the reaction between magnesium ferrite and potassium carbonate. By itself potassium carbonate is stable up to its melting point at 1164 K (*30*). In the presence of magnesium ferrite, however, potassium carbonate starts to decompose at 923 K. Thermodynamically, this process is driven by the formation of a mixed oxide of

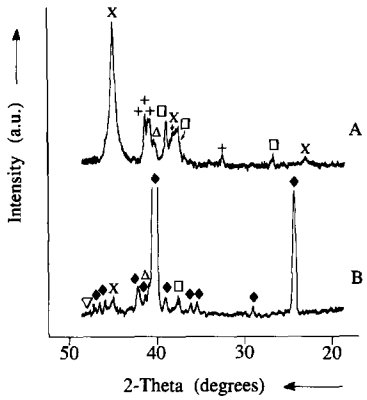

FIG. 7. X-ray diffractograms of a 1 : 1 (wt/wt) $MgFe_2O_4/K_2CO_3$ mixture before (A) and after (B) calcination in air at 1073 K. (▽) MgO, (X) $MgFe_2O_4$, (□) K_2SO_4, (+) $K_2CO_3 \cdot \frac{3}{2}H_2O$, (△) K_2CO_3, (◆) $KFeO_2$.

potassium and iron. A similar effect has also been observed for potassium carbonate in the presence of α-Fe_2O_3 (*34–37*). Dvoretskii *et al.* (*35*) and Subrt *et al.* (*36*) observed the formation of $KFeO_2$ from α-Fe_2O_3 and K_2CO_3 in air at temperatures between 873 and 1073 K. In the temperature range from 1123 to 1233 K, $KFeO_2$, potassium (mono)-ferrite, was found to react subsequently with an excess of α-Fe_2O_3 to form potassium polyferrites according to (*35, 36*):

$$K_2CO_3 + \alpha\text{-}Fe_2O_3 \rightarrow 2KFeO_2 + CO_2\uparrow \quad (2)$$

$$2KFeO_2 + (n-1)\alpha\text{-}Fe_2O_3 \rightarrow K_2O \cdot nFe_2O_3 \quad (3)$$

As the α-Fe_2O_3 is more dispersed, the reaction to $KFeO_2$ is reported to be more extensive (*37*). According to Plyasova *et al.* (*38*), $KFeO_2$ is formed from α-Fe_2O_3 already at 723 K in the presence of steam. The reactivity of γ-Fe_2O_3 toward K_2CO_3 has been reported to be higher, if compared with that of α-Fe_2O_3 (*39*). The formation of potassium polyferrites, such as those reported in the literature, e.g., $KFe_{11}O_{17}$ (*33*), KFe_5O_8 (*40*), and $K_2Fe_{12}O_{19}$ (*40*), is not observed in this research. This is to be expected, since neither the supported catalysts nor the $MgFe_2O_4/K_2CO_3$ bulk mixture described in this work has been calcined at temperatures as high as 1123 K. In addition, according to reaction Eq. (3), substantial formation of potassium polyferrites would require the presence of an excess of magnesium ferrite.

A remarkable feature of the olive-green $KFeO_2$ phase, which has been formed during calcination of the $MgFe_2O_4/K_2CO_3$ mixture at 1073 K in air, is that it rapidly turns brown upon exposure to atmospheric air at room temperature. Within 3 h the green color has totally disappeared. Upon exposure to air, which had been partially saturated with water, the effect is exhibited much faster. The literature is not unequivocal about this phenomenon. According to Pistorius and de Vries (*28*), $KFeO_2$ is merely hygroscopic. Others argue that at room temperature in air, mainly under the influence of water and carbon dioxide, $KFeO_2$ decomposes to α-Fe_2O_3 and various potassium carbonates (*20, 38, 41*). Scholder and Mansmann (*33*), on the other hand, claimed their potassium ferrites to be stable in air. To clarify the phenomenon, X-ray diffraction has been performed on $KFeO_2$ after exposure to air at room temperature and after subsequent recalcination at 773 K. The X-ray diffractograms are shown in Fig. 8. The diffractogram of the fresh $KFeO_2$ sample (A), which has been recorded directly after calcination of the $MgFe_2O_4/K_2CO_3$ mixture at 1073 K, shows $KFeO_2$ diffraction lines. This diffractogram is the same as the one shown in Fig. 7B. Upon 3 h of exposure to atmospheric air at room temperature (B) the intensities of the $KFeO_2$ diffractions have strongly diminished. After 24 h of exposure (C) the effect is even more pronounced. The $KFeO_2$ diffraction at 2θ = 24.3° has completely disappeared. Additionally, potassium carbonate diffractions have reappeared. Also a new diffraction has appeared at 2θ = 30.6°. This diffraction with

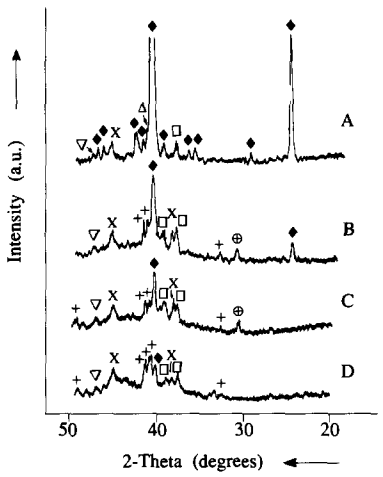

FIG. 8. X-ray diffractograms of a 1:1 (wt/wt) $MgFe_2O_4/K_2CO_3 \cdot \frac{3}{2}H_2O$ mixture after various subsequent treatments. (A) Calcination at 1073 K; (B) exposure to atmospheric air, 3 h; (C) exposure to atmospheric air, 24 h; (D) recalcination at 773 K. (▽) MgO, (X) $MgFe_2O_4$, (□) K_2SO_4, +: $K_2CO_3 \cdot \frac{3}{2}H_2O$, (△) K_2CO_3, (◆) $KFeO_2$, (⊕) $KHCO_3$.

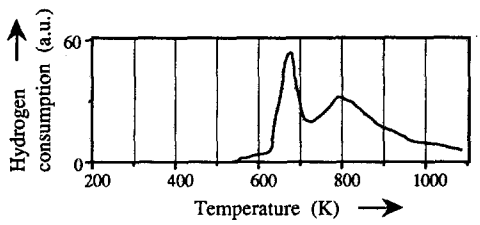

FIG. 9. TPR profile of a 4.5 wt% Fe/MgO catalyst (*25*).

d = 3.67 Å is typical of potassium hydrogen carbonate, $KHCO_3$. If the change in color were due merely to hydration of $KFeO_2$, then, upon calcination at 773 K (which is below the temperature of $KFeO_2$ formation) to remove hydrate water, the $KFeO_2$ diffractions should be regained. However, as can be seen in diffractogram D, this does not happen. Instead, the $KFeO_2$ diffraction at 2θ = 40.2° has become even weaker, yet it has not disappeared completely. Upon calcination at 773 K the $KHCO_3$ diffraction vanishes, whereas the $K_2CO_3 \cdot \frac{3}{2}H_2O$ diffractions become more intense. This can be explained by the fact that potassium hydrogen carbonate decomposes into potassium carbonate, carbon dioxide, and water at temperatures between 373 and 473 K (*42*). The formation of potassium carbonate and potassium hydrogen carbonate suggests that $KFeO_2$ is indeed decomposed at room temperature. With X-ray diffraction, however, no diffractions belonging to iron compounds other than those of $KFeO_2$ or $MgFe_2O_4$ are detected, as was found by others (*20, 38, 41*). It is self-evident that $MgFe_2O_4$ is not a decomposition product. Probably some amorphous hydrated form of iron oxide, such as α-FeOOH, is formed upon exposure to atmospheric air. Only upon calcination at temperatures above 923 K is $KFeO_2$ obtained again.

Summarizing, $KFeO_2$ is not stable in atmospheric air and decomposes under the influence of water vapor and carbon dioxide to potassium hydrogen carbonate, potassium carbonate, and presumably a (hydrated) iron oxide.

Reduction Behavior

To determine the effect of potassium promotion on the reduction behavior, the promoted catalysts have been studied using TPR.

Previously, it has been shown magnetically that unpromoted Fe/MgO catalysts are reduced under dehydrogenation conditions (*2*). In a 1-butene/steam/nitrogen feed at 873 K, the magnesium ferrite phase in the unpromoted catalyst is reduced to FeO and partly also to Fe_3O_4. In a separate study of the reduction behavior of unpromoted Fe/MgO catalysts using both TPR and magnetic measurements (*26*), it was found that in a 10% H_2/Ar flow $MgFe_2O_4$ is reduced in two steps. Figure 9 shows the TPR profile of an unpromoted 4.5 wt% Fe/MgO catalyst, which is typical of the reduction of $MgFe_2O_4$. In the first step, viz., between 550 and 723 K, $MgFe_2O_4$ is reduced, partly via Fe_3O_4, to FeO, which is dissolved in the MgO support. In the second step, which starts at about 723 K, FeO is reduced further to metallic iron.

The effect of potassium promotion is shown in Fig. 10. TPR profiles of a 3 wt% Fe/MgO catalyst consecutively impregnated with potassium carbonate were re-

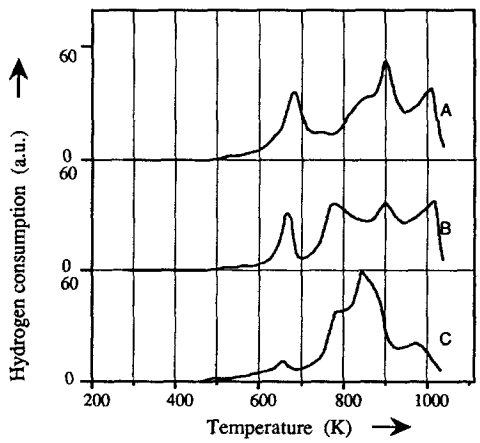

FIG. 10. TPR profiles of a 3 wt% Fe/MgO catalyst promoted with 3 wt% K using the consecutive method and calcined at various temperatures. (A) 393 K, (B) 873 K, (C) 973 K.

corded after drying at 393 K (A), after calcination at 873 K (B), and after calcination at 973 K (C). The phase compositions of these catalysts, as determined using X-ray diffraction, have been discussed above (Fig. 3). It has been observed that the catalyst after drying at 393 K contains magnesium ferrite, potassium sulfate, and potassium carbonate. Accordingly, the TPR profile in Fig. 10A shows four reduction peaks. The first reduction peak, starting at about 550 K, as observed in the unpromoted catalyst in Fig. 9, corresponds to reduction of $MgFe_2O_4$ to FeO. The second reduction peak, i.e., reduction of FeO to metallic iron, is present also as a broad peak starting at about 773 K. Compared with the unpromoted catalyst, the only difference is that this second reduction step has shifted to higher temperatures. This can be explained by the hydroxylation of the MgO support to form $Mg(OH)_2$ during the impregnation. In the course of the TPR, large amounts of water evolve, starting at about 700 K, due to the decomposition of $Mg(OH)_2$ (*27*). The high water vapor concentration is very effective in retarding reduction of FeO to metallic iron. Superimposed onto this broad second reduction peak are two separate reductions, the areas of which are not related to the presence of iron in any way. The first one, between 870 and 950 K, is the reduction of potassium sulfate, as has been experimentally determined separately. In the unpromoted catalyst the sulfate is present also, only as magnesium sulfate. The latter is reduced in the same temperature range (*26*). However, reduction of magnesium sulfate in the unpromoted catalyst does not result in such sharp and clearly observable reduction peaks as does reduction of potassium sulfate. According to Zyryanov *et al.* (*43*), potassium sulfate is reduced to potassium sulfide, K_2S. Therefore a small amount of potassium sulfate results in a relatively large hydrogen consumption. The final peak at 1000 K is linked with reduction of carbonate to, for example, carbon monoxide or methane. For bulk K_2CO_3, reduction of carbonate does not proceed at this temperature. Metallic iron, which is present as a result of the reduction of magnesium ferrite, may act as a catalyst for the reduction of carbonate.

After calcination at 873 K, X-ray diffraction has shown (Fig. 3) that $Mg(OH)_2$ has been decomposed. Accordingly, in Fig. 10B, the second reduction peak of $MgFe_2O_4$ has shifted back to its original position at about 780 K. The position of the two final reduction peaks remains unaltered. The area of the sulfate peak seems to have decreased. Although difficult to quantify, this apparent decrease is caused by shifting of the $MgFe_2O_4$ reduction peak to lower temperatures. After calcination at 973 K, the TPR profile has changed drastically. With XRD, TMA, and TGA it was observed that upon calcination at 973 K $MgFe_2O_4$ reacts with K_2CO_3 to form $KFeO_2$. Accordingly, the first reduction peak in Fig. 10C, viz., that of $MgFe_2O_4$, has almost disappeared, while the final peak due to reduction of carbonate has decreased due to reaction to $KFeO_2$. The second reduction peak, at about 780 K, remains present. Evidently, this peak now originates from reduction of $KFeO_2$ in one step to metallic iron. Consequently, the initially present first and second reduction peaks in profile B, viz., those of $MgFe_2O_4$, must have coalesced to one $KFeO_2$ reduction peak starting at about 770 K. The reduction peak of potassium sulfate is still present; only its shape has changed due to the changed position of the iron reduction peaks.

The effect of the amount of potassium promoter has been studied also. For this purpose TPR profiles were recorded for a 3 wt% Fe/MgO catalyst containing 1, 3, and 6 wt% K, as shown in Figs. 11A, 11B, and 11C, respectively. All catalysts have been previously calcined in air at 973 K. The phase compositions of these catalysts have been discussed above. In the catalyst containing 1 wt% K (A), the amount of potassium is far too low to accomplish full conversion of $MgFe_2O_4$ into $KFeO_2$. As a result the two magnesium ferrite reduction

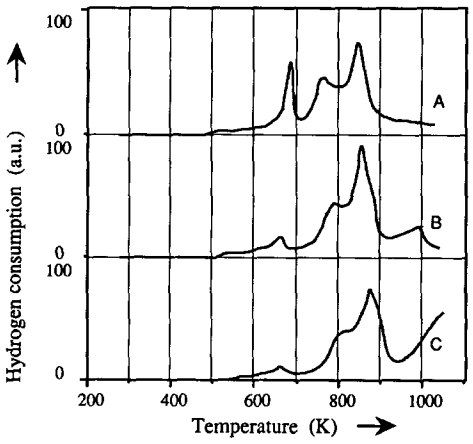

FIG. 11. TPR profiles of a 3 wt% Fe/MgO catalyst consecutively promoted with different amounts of potassium. The catalysts have been calcined at 973 K. (A) 1 wt% K, (B) 3 wt% K, (C) 6 wt% K.

peaks are still clearly present. Again the sulfate reduction peak is visible. The reduction peak of carbonate, however, is practically absent. The small amount of potassium carbonate brought onto the catalyst by impregnation has evidently reacted mainly to K_2SO_4. The TPR profile of the catalyst containing 3 wt% K (B), which is a slight excess regarding $KFeO_2$ formation, clearly shows the presence of potassium carbonate. With XRD it has been established that here magnesium ferrite has reacted almost quantitatively to $KFeO_2$ (Fig. 4). Accordingly, the first reduction peak of $MgFe_2O_4$ has almost vanished. Again, as was also seen in Fig. 10C, the second reduction peak remains present as a reduction peak of $KFeO_2$. A large excess of potassium, as with 6 wt% K in Fig. 11C, has a minor influence on the conversion of magnesium ferrite into potassium ferrite. The excess of potassium results in a proportionally larger reduction peak of carbonate. In these TPR profiles the area of the sulfate reduction peak remains unaltered. Increasing the amount of potassium from 1 to 6 wt% results in a shift of the second reduction peak of about 30 K to higher temperatures, along with the conversion of magnesium ferrite into potassium ferrite.

It must be concluded that the onset of reduction of iron oxide, initially present as magnesium ferrite, is strongly retarded by the formation of a mixed oxide with potassium. The onset temperature of reduction of $KFeO_2$ is about 200 K higher than that of reduction of magnesium ferrite.

With X-ray diffraction it was observed that $KFeO_2$ decomposes in atmospheric air to form potassium carbonate, potassium hydrogen carbonate, and a (hydrated) iron oxide. Since the formation of potassium ferrite has such a retarding effect on the reduction of iron oxide, the decomposition is expected to have a large effect on the TPR profile. Figure 12 shows the TPR profiles of a 3 wt% Fe/MgO catalyst promoted with 3 wt% K, before (A) and after (B) exposure to atmospheric air at room temperature for 500 h. The fresh catalyst still contains some unreacted magnesium ferrite next to potassium ferrite. Also, reductions of potassium sulfate and potassium carbonate are observable. Remarkably, exposure to atmospheric air for 500 h had only a minor influence on the TPR profile, despite the decomposition of $KFeO_2$. In accordance with the XRD results, shown in Fig. 8, the amount of potassium carbonate has slightly increased. However, the position and the relative sizes of the iron oxide reduction peaks remain unchanged. The only further important dif-

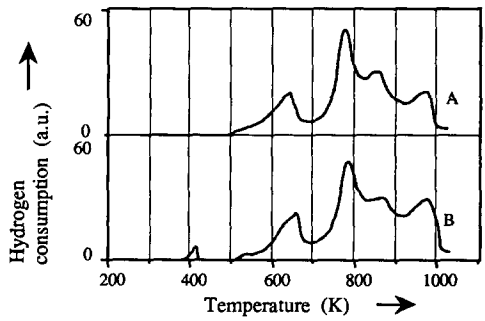

FIG. 12. TPR profiles of a 3 wt% Fe/MgO catalyst consecutively promoted with 3 wt% potassium (A) before and (B) after exposure to atmospheric air for 500 h.

ference is the appearance of a small peak at about 400 K. This peak cannot be related to water desorbing from the catalyst, because water is frozen out using a CO_2 cold trap. Also the peak is observed at too low a temperature to be attributed to an iron oxide reduction. The only plausible explanation is that it originates from the decomposition of potassium hydrogen carbonate formed during exposure to air. Upon decomposition of the potassium hydrogen carbonate carbon dioxide and water evolve, of which the carbon dioxide evidently is not frozen out.

CONCLUSIONS

Impregnation of magnesium oxide with a solution of both potassium carbonate and an iron precursor, such as ammonium iron(III) citrate or ammonium iron(III) EDTA, results in homogeneous distributions of both iron and potassium throughout the magnesium oxide support pellets. Impregnation afterwards of iron oxide catalysts supported on magnesium oxide with a solution containing potassium carbonate also results in a homogeneous distribution of potassium. However, in this case potassium sulfate deposits were found at the external edge of the catalyst pellets after drying. The sulfate originates from the MgO support (*27*). Potassium sulfate deposits on the external edges of the pellets are absent for the simultaneously impregnated catalysts. This is related to the presence of badly crystallizing iron complexes during the drying step, which inhibits the transport of the impregnation solution (*23*).

Upon calcination beyond 923 K, promotion of iron oxide catalysts supported on magnesium oxide with potassium results in the formation of a mixed oxide of potassium and iron, viz., $KFeO_2$. This was unambiguously demonstrated using XRD, TMA, and TGA. As determined using X-ray line broadening, the average crystallite size of the $KFeO_2$ phase is 300 Å. The larger crystallite radius compared to the initial magnesium ferrite crystallite radius, which is about 230 Å as determined using oxygen chemisorption (*32*), can be explained by a lattice expansion of the mixed iron oxide due to the incorporation of the relatively large K^+ ion instead of the Mg^{2+} ion. Moreover, solely on the basis of the difference in densities between $MgFe_2O_4$ and $KFeO_2$, which are 4.5 and 3.36 g/cm^3 respectively, and the initial $MgFe_2O_4$ crystallite size of 230 Å, a $KFeO_2$ crystallite size of 280 Å would be expected. This agrees well with the value of 300 Å found using XRD. Nevertheless, since X-ray diffraction was performed in air, care should be taken with the interpretation of X-ray line broadening. After all, the peak width may be influenced by decomposition of $KFeO_2$ in air.

Other mixed oxides, the so-called potassium polyferrites reported in the literature, were not observed (*35, 36*). Furthermore, no reaction between potassium ions and the magnesium oxide support was established, as is in agreement with Perrichon and Durupty (*44*). Whereas potassium is known to react extensively with supports, such as Al_2O_3 and SiO_2, no mixed oxides of potassium and magnesium are known.

Temperature-programmed reduction showed that $KFeO_2$ is reduced to metallic iron in one single reduction step. $KFeO_2$ has turned out to be far more difficult to reduce than $MgFe_2O_4$. Whereas reduction of $MgFe_2O_4$ to FeO starts at about 600 K, $KFeO_2$ is not reduced in hydrogen below 770 K. Although they did not actually report the presence of potassium ferrite, retardation of reduction of iron oxide by the presence of potassium has also been observed by Moral *et al.* (*45*). Dejaifve *et al.* (*21*) reported that potassium polyferrite, e.g., $K_2Fe_{12}O_{19}$, is more easily reducible than $KFeO_2$. Evidently retardation of reduction is not as strong for potassium polyferrites as it is for $KFeO_2$.

In atmospheric air potassium ferrite was found to decompose due to reaction with carbon dioxide and moisture. After decomposition, carbonates, such as $K_2CO_3 \cdot \frac{3}{2}H_2O$ and $KHCO_3$, have been formed. As a result, iron oxide, probably α-FeOOH, should also

have been formed. However, this phase was X-ray amorphous and was not detectable using X-ray diffraction. Moisture has been found to enhance the decomposition of $KFeO_2$ at room temperature. In light of this fact, it is remarkable that water vapor is also reported to have an accelerating effect on the formation of $KFeO_2$ from α-Fe_2O_3 and K_2CO_3 at high temperatures (*38*). The decomposition of $KFeO_2$ upon exposure to air does not have a major effect on the reduction behavior. Evidently, the degree of interaction between iron oxide and the alkali promotor is maintained to such an extent that the reduction of the iron oxide does not become more facile.

From the instability of potassium ferrites toward carbon dioxide and moisture, it is learned that strict precautions should be taken to avoid contact of the catalysts with atmospheric air. It is probably for this reason that several authors did not observe the presence or the formation of a mixed oxide of potassium and iron (*46–50*). The prevention of contact with atmospheric air is especially important when the phase composition of the catalyst during dehydrogenation conditions is studied. In that case *in situ* techniques would be required (*51*).

In the succeeding paper the behavior of the supported iron oxide catalyst promoted with potassium in the dehydrogenation of 1-butene will be described. The phase composition under dehydrogenation conditions is characterized (*22*).

REFERENCES

1. Stobbe, D. E., Ph.D. thesis, Utrecht (1990).
2. Stobbe, D. E., van Buren, F. R., Hoogenraad, M. S., van Dillen, A. J., and Geus, J. W., *J. Chem. Soc. Faraday Trans.* **87,** (10) 1639 (1991).
3. Buyanov, R. A., Chesnokov, V. V., Afanas'ev, A. D., and Babenko, V. S., *Kinet. Catal.* **18,** 839 (1977).
4. Afanas'ev, A. D., Buyanov, R. A., and Chesnokov, V. V., *Kinet. Catal.* **23,** 1042 (1982).
5. Babenko, V. S., Buyanov, R. A., and Afanas'ev, A. D., *Kinet. Catal.* **23,** 105 (1982).
6. Babenko, V. S., Buyanov, R. A., and Afanas'ev, A. D., *Kinet. Catal.* **23,** 827 (1982).
7. Babenko, V. S., and Buyanov, R. A., *Kinet. Catal.* **27,** 441 (1986).
8. Hirsch, R. L., Gallagher, J. E., Lessard, R. R., and Wesselhoff, R. D., *Science* **215,** 121 (1982).
9. Mross, W.-D., *Catal. Rev.-Sci. Eng.* **25,** 591 (1983).
10. Lee, E. H., *Catal. Rev.* **8,** 285 (1973).
11. Lee, E. H., and Holmes, L. H., Jr., *J. Phys. Chem.* **67,** 947 (1963).
12. Vijh, A. K., *J. Chim. Phys.* **72,** 5 (1975).
13. Muhler, M., Schlögl, R., and Ertl, G., *Surf. Interface Anal.* **12,** 233 (1988).
14. Muhler, M., Schlögl, R., and Ertl, G., *in* "Proceedings, 9th International Congress on Catalysis, Calgary, 1988" (M. J. Phillips and M. Ternan, Eds.), Vol. 4, p. 1758. Chem. Institute of Canada, Ottawa, 1988.
15. Courty, P., and Le Page, J. F., *in* "Preparation of Catalysts" (B. Delmon, P. Grange, P. Jacobs, and G. Poncelet Eds.), Vol. II, Studies in Surface Science and Catalysis, Vol. 3, p. 293. Elsevier, Amsterdam 1979.
16. Dry, M. E., and Ferreira, L. C., *J. Catal.* **7,** 352 (1967).
17. Shibata, K., and Kiyoura, T., *Bull. Chem. Soc. Jpn.* **42,** 871 (1969).
18. Hirano, T., *Appl. Catal.* **26,** 81 (1986).
19. Molchanov, V. V., Andrushkevich, M. M., Plyasova, L. M., and Kotel'nikov, G. R., *Kinet. Catal.* **29,** 1107 (1988).
20. Muhler, M., Schlögl, R., Reller, A., and Ertl, G., *Catal. Lett.* **2,** 201 (1989).
21. Dejaifve, P. E., Darnanville, J.-P., Garin, R. A. C., Clement, J. C., and Lambert, J. C., EP A-0,339,704 (1989).
22. Stobbe, D. E., van Buren, F. R., van Dillen, A. J., and Geus, J. W., *J. Catal.* **135,** 548 (1992).
23. Stobbe, D. E., van Buren, F. R., Stobbe-Kreemers, A. W., Schokker, J. J., van Dillen, A. J., and Geus, J. W., *J. Chem. Soc. Faraday Trans.* **87**(10), 1623 (1991).
24. Selwood, P. W., "Chemisorption and Magnetization." Academic Press, New York, 1975.
25. Kock, A. J. H. M., de Bokx, P. K., Boellaard, E., Klop, W., and Geus, J. W., *J. Catal.* **96,** 468 (1985).
26. Stobbe, D. E., van Buren, F. R., Stobbe-Kreemers, A. W., van Dillen, A. J., and Geus, J. W., *J. Chem. Soc. Faraday Trans.* **87**(10), 1631 (1991).
27. Stobbe, D. E., van Buren, F. R., Groenendijk, P. E., van Dillen, A. J., and Geus, J. W., *J. Mater. Chem.* **1**(4), 539 (1991).
28. Pistorius, C. W. F. T., and de Vries, G. F., *Z. Anorg. Allg. Chem.* **395,** 119 (1973).
29. Barth, T. F. W., *J. Chem. Phys.* **3,** 323 (1935).
30. Weast, R. C. (Ed.), "Handbook of Chemistry and Physics," 62nd ed., B-131/B-137. CRC Press, Boca Raton, FL, 1981.
31. Schieber, M. M., *in* "Selected Topics in Solid State

Physics" (E. P. Wohlfarth, Ed.), Vol. 8. North-Holland, Amsterdam, 1967.
32. Stobbe, D. E., van Buren, F. R., Orbons, A. J., van Dillen, A. J., and Geus, J. W., *J. Mater. Sci.*, **27,** 343 (1992).
33. Scholder, R., and Mansmann, M., *Z. Anorg. Allg. Chem.* **321,** 246 (1963).
34. Plyasova, L. M., Andrushkevich, M. M., Kotel'nikov, G. R., Buyanov, R. A., Khramova, G. A., Kustova, G. N., and Villert, M. V., *Kinet. Catal.* **17,** 654 (1976).
35. Dvoretskii, N. V., Stepanov, E. G., Sudzilovskaya, T. N., Kotel'nikov, G. R., and Yun, V. V., *Inorg. Mater.* **25,** 242 (1989).
36. Subrt, J., Vins, J., Shaplygin, I. S., and Zakharov, A. A., *Thermochim. Acta* **93,** 489 (1985).
37. Molchanov, V. V., Andrushkevich, M. M., Plyasova, L. M., Buyanov, R. A., and Kotel'nikov, G. R., *Kinet. Catal.* **29,** 218 (1988).
38. Plyasova, L. M., Andrushkevich, M. M., Kotel'nikov, G. R., Buyanov, R. A., Khramova, G. A., Kustova, G. N., and Bednov, S. F., *Kinet. Catal.* **17,** 1116 (1976).
39. Mihajlova, A., Andreev, A., Shopov, D., and Dimitrova, R., *Appl. Catal.* **40,** 247 (1988).
40. Rooymans, C. J. M., Langereis, C., and Schulkes, J. A., *Solid State Commun.* **4,** 85 (1965).
41. Andrushkevich, M. M., Plyasova, L. M., Molchanov, V. V., Buyanov, R. A., Kotel'nikov, G. R., and Abramov, V. K., *Kinet. Catal.* **19,** 332 (1978).
42. Schmitt, K. O., *Z. Anal. Chem.* **70,** 321 (1927).
43. Zyryanov, S. I., Ibragimov, V. A., Rozovskii, A. Ya., and Mostinskii, I. L., *Kinet. Catal.* **28,** 930 (1987).
44. Perrichon, V., and Durupty, M. C., *Appl. Catal.* **42,** 217 (1988).
45. Moral, P., Praliaud, H., and Martin, G.-A., *React. Kinet. Catal. Lett.* **34,** 1 (1987).
46. Pospisil, M., Spevacek, J., and Kryska, J., *Coll. Czech. Chem. Commun.* **48,** 421 (1983).
47. Sayyed, B. A., Gupta, M. P., Date, S. K., Kamble, K. R., Sonsale, A. Y., and Chatterjee, A. K., *Proc. Indian Acad. Sci. (Chem. Sci.)* **95,** 285 (1985).
48. Sayyed, B. A., Chatterjee, A. K., Kanetkar, S. M., Badrinarayanan, S., and Date, S. K., *Proc. Indian Acad. Sci. (Chem. Sci.)* **95,** 291 (1985).
49. Chen, S. J., and Sheu, F. C., *Proc. 3rd Pac. Chem. Eng. Congr.* **2,** 268 (1983).
50. Kaushik, V. K., Prasada Rao, T. S. R., Yadav, B. L. S., and Chhabra, M. S., *Appl. Surf. Sci.* **32,** 93 (1988).
51. Muhler, M., Schlögl, R., Eder, S., and Ertl, G., *Surf. Sci.* **189/190,** 69 (1987).